International Journal of Botany Studies
ISSN: 2455-541X
Impact Factor: RJIF 5.12
www.botanyjournals.com
Volume 2; Issue 5; September 2017; Page No. 71-75

Green synthesis of Manganese nanoparticles using the aqueous extract of *Ctenolepis garcini* (Burm. f.) C.B Clarke

[*1] J John Peter Paul, [2] M Sakunthala, [3] C Iniya Udhaya

[1] Assistant Professor & Director, Centre for Advanced Research in Plant Sciences (CARPS), Department of Botany, St. Xavier's College (Autonomous), Palayamkottai, Tamil Nadu, India

[2, 3] Research Scholar, Centre for Advanced Research in Plant Sciences (CARPS), Department of Botany, St. Xavier's College (Autonomous), Palayamkottai, Tamil Nadu, India

Abstract
In the present report, a novel biological approach for the formation of Manganese nanoparticles using *Ctenolepis garcinii* (Burm.f.) C.B Clarke was described. Manganese was made to reduce with aqueous solution of plant extracts to form the manganese nanoparticles. UV-Visible spectrum showed the characteristic absorption peak of manganese nanoparticles at 415-417nm. Fourier Transform Infra-Red (FTIR) spectrum and X-Ray diffraction (XRD) pattern revealed the formation of manganese nanoparticles, while Energy Dispersive X-ray microanalysis spectroscopy (EDX) and Scanning Electron Microscopy (SEM) suggested the particles size and shape in the range of 57-69nm. SEM image also revealed the manganese particles are spherical and granular nature.

Keywords: manganese nanoparticles, UV-Visible, FTIR, XRD, EDX, SEM

1. Introduction
Nanobiotechnology is a new area of increasing research and industrial interest for past few decades. Nanobiotechnology can be defined as the manipulation of atom by atom from the material world by the combination of engineering, chemical and biological approaches. Nanoparticles exhibit unique physical and chemical properties compared with their bulk materials. There is significant interest in obtaining well-dispersed, ultrafine and uniform nanoparticles to delineate and utilise their distinct properties (Lee *et al*., 2014) [1]. The unique size-dependent properties and excellent process ability of colloidal metal oxide make potential candidates for technological applications. Colloidal and supported metal nanomaterials have been used as catalysts in several reactions such as oxidations (Kabir *et al*., 2008) [2], cross-coupling reactions (Gopidas *et al*., 2003) [3], electron transfer reactions (Sharma *et al*., 2003) [4], hydrogenations (Boudjahem *et al*., 2004) [5] and fuel cell reactions (Moore *et al*., 2003) [6].
A multiple of research have established that zinc oxide, manganese oxide nanoparticles have antifungal and antibacterial activity. The other metal nanoparticles like silver nanoparticles also carry these properties. Recent inspiring improvements in the field of nanotechnology have been observed because of development of different and efficient methodologies to fabricate nanoparticles of particular shape and size depending on the specific requirements. Nanobiotechnology is a science and engineering branch of recently well-established technology referring at the nanoscale, i.e., 1 to 100nm. In the recent years, the various size and shape of different nanomaterials has been realized through a wet-chemical synthesis because of its wide range of application.
Due to this reason, researchers try to develop an increasing interest to fabricate nanostructured materials. Owing to the variable oxidation states, manganese oxides have attracted substantial attention, because of the superior magnetic, electrical and chemical properties which promise great potential in superconductivity applications. In recent years, considerable research has been focused on nanostructured manganese oxides. It has been well documented that nanostructured manganese oxides possess unique magnetic (Nayak and Jena, 1999) [7]. Nano-MnO_2 has great potential applications in environment protection field as a new generation of environmental friendly catalyst. In this background, the present work was indented to prepare and characterize the manganese nanoparticles using the aqueous extract of *Ctenolepis garcinii* (Burm.f.) C.B Clarke.

2. Materials and methods
2.1. Collection of plant materials
The plant material used in the present study is *Ctenolepis garcinii* (Burm. f.) C.B. Clarke belonging to the family Cucurbitaceae. *Ctenolepis garcinii* (Burm. f.) C.B. Clarke was collected near to Manonmaniam Sundaranar University, Tirunelveli, located in Tirunelveli district, Tamil Nadu, India during the month of December, 2015 and identified and confirmed by the flora of the Presidency of Madras (Gamble, 1919).

2.2. Synthesis of manganese nanoparticles
2g air dried *Ctenolepis garcinii* (Burm. f.) C.B. Clarke powder was taken in a 100ml Erlenmeyer flask with 30ml of sterile

distilled water and then boiled the mixture for 2 minutes. After boiling, the mixture was filtered in the Whatmann No.1 filter paper. 1mM solution of potassium permanganate was prepared. 5ml of plant extract was mixed with 25ml of 1mM potassium permanganate solution. The formation of red colour was observed and λ max at different time intervals were taken for 8h using a UV-Visible spectroscopy. The solution is stored in room temperature for 24h for the complete settlement of nanoparticles. After 24h centrifuge the reaction mixture, discard the supernatant. Add 1ml of distilled water to the pellet and wash by using centrifugation. Collect the pellet by using acetone/ethyl acetate/alcohol. Dry in the watch glass and store the nanoparticles (Frattini *et al*., 2005) [8].

2.3. Characterization of manganese nanoparticles

UV-Visible spectra analysis

The reduction of pure manganese ions was observed by measuring the UV-Visible spectrum of the reaction at different time intervals by taking 2ml of the sample compared with 2ml of 1mM potassium permanganate solution respectively used as blank. UV-Visible spectral analysis has been one by using an Elico spectrophotometer at a resolution of 1nm from 200 to 1100nm (Iniya Udhaya *et al.,* 2015) [9].

FT-IR analysis

FT-IR spectrum in the range 4000 to 400cm^{-1} at a resolution of 4cm^{-1} using Perkin-Elmer spectrometer was used to detect the manganese nanoparticles. The sample was mixed with KCl procured from Sigma. Thin sample disc was prepared by pressing with the disc preparing machine and placed in Fourier Transform Infra Red (FTIR) for the analysis of the nanoparticles (John Peter Paul and Shri Devi, 2014) [10].

XRD analysis

X-ray diffraction (XRD) analysis of drop-coated films of the manganese nanoparticles in sample was prepared for the determination of the formation of manganese nanoparticles by XPERT-PRO software and X-ray diffractometer operated at a voltage of 40kv and a current of 30mA with Mn Kα radiation (Muthu Sheeba *et al.,* 2014) [11].

SEM and EDX analysis

The structure, composition and average size of the synthesized manganese, nanoparticles were analyzed by Scanning Electron Microscopy and Energy Dispersive X-ray microanalysis spectroscopy (EDX, Sigma). Scanning Electron Microscope (SEM) analysis was made using VEGA3 TESCAN SEM machine. After the preparation of the manganese nanoparticles, thin films of the suspension of the manganese nanoparticles were extra solution was removed using a blotting paper and then the film on the SEM grid were allowed to dry by putting it under a mercury lamp for 5 minutes, followed by SEM observations were carried out (Sakunthala *et al.,* 2017) [12].

3. Results & Discussion

3.1. Synthesis of manganese nanoparticles

Reduction of manganese ion into manganese particles during exposure to the plant extract could be followed by colour change. Manganese nanoparticles exhibited red colour from violet in aqueous solution due to the surface Plasmon resonance phenomenon. The appearance of the red colour (Fig.1) indicated the formation of manganese nanoparticles in the reaction mixture, as it was well known that manganese nanoparticles exhibited striking colours (violet to red) due to excitation of surface plasmon vibrations in the particles. It was reported that some amount of OH- groups tended to promote the reduction of manganese ions in some chemical methods.

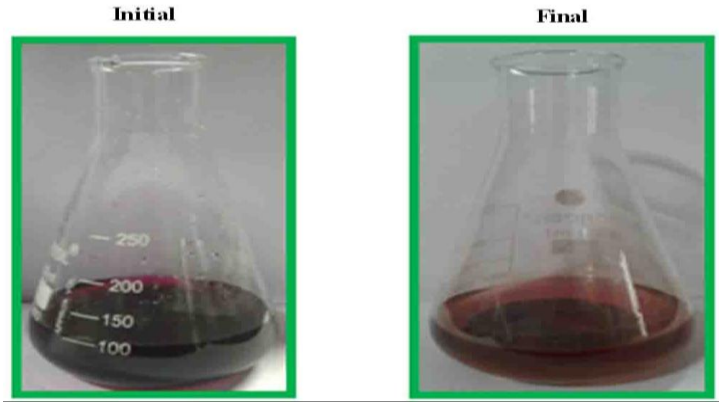

Fig 1: Formation of MnNPs using *Ctenolepis garcinii* (Burm.f.) C.B. Clarke.

3.2. UV-Visible spectrum

UV-Visible spectra of the reaction media were taken at different time intervals explicit that the Surface Plasmon Resonance (SPR) vibrations were found between 415 to 417nm with λmax at 417nm with absorption of 0.026 which was dark green colour shifted. The brown colour shifted at 415.5nm with absorption of 0.104, followed by light green colour at 416.5nm with absorption of 0.089, orange colour at 415.5nm with absorption of 0.104, followed by red colour 415nm with absorption of 0.171 was related to an increase the amount of manganese nanoparticles (Fig.2). The position and the number of peaks in the absorption spectra were dependent on the shape of the particles. For an ellipsoidal particle there are two peaks whereas for spherical particle there was only one peak (Creighton and Eadont, 1991) [13]. In the present study, there is only one peak at the centre indicating the formation of manganese nanoparticles in spherical shape. The absorption maximum at 417nm was attributed to the Mie

scattering by magnesium metal (Aoki *et al.*, 2003) [14].

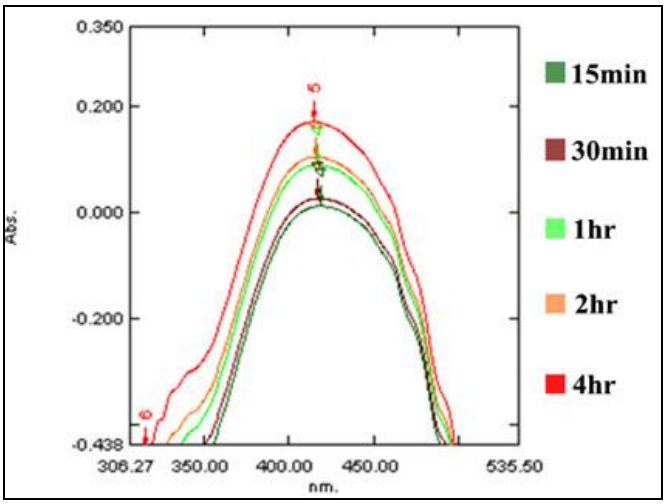

Fig 2: UV-Visible spectrum of MnNPs using *Ctenolepis garcinii* (Burm.f.) C.B. Clarke.

3.3. FT-IR spectrum

FT-IR spectrum of manganese nanoparticles was shown in Fig.3 and Table-1. This spectrum showed the presence of bands at 513.03, 620.07, 989.41, 1130.21, 1194.82, 1383.83, 1562.23 1648.06, 2881.45, 3299.01 and 3515.99cm^{-1}. The bands at 513.03cm^{-1} corresponds to amines (C-N-C bend), 620.07cm^{-1} to ketones (C-CO-C bend), 989.41 was assigned to vinyl compounds (CH deformation), the band at 1130.21cm^{-1} was assigned to primary aliphatic amines (C-N stretch), 1194.82cm^{-1} to thiocarbonyl compounds (C=S stretch), 1383.83cm^{-1} corresponds to sulfonyl chlorides (SO_2 antisym stretch), 1562.23cm^{-1} to secondary amides (NH deformation), 1648.06cm^{-1} corresponds to primary amides (NH deformation) 2881.45cm^{-1} to aliphatic compounds (CH stretch), 3299.01cm^{-1} to amino acids (NH_3 stretch) and 3515.99cm^{-1} to aromatic amines (NH stretch). The positions of these bands were close to that reported for native proteins (Kapoor, 1998) [15]. This evidence suggests that the protein molecules could possibly perform the function of the formation and stabilization of manganese nanoparticles in the aqueous medium.

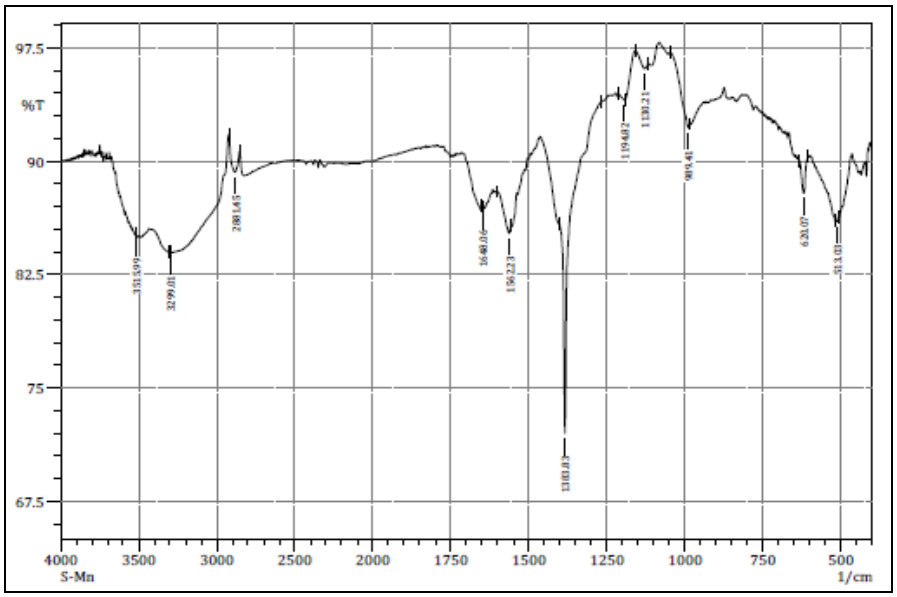

Fig 3: FTIR spectrum of MnNPs using *Ctenolepis garcinii* (Burm.f.) C.B. Clarke.

Table 1: FTIR peak value of MnNPs using *Ctenolepis garcinii* (Burm.f.) C.B. Clarke

Peak Value	Functional group	Assignments
513.03	C-N-C in amines	C-N-C bend
620.07	C-CO-C in ketones	C-CO-C bend
989.41	CH-CH_2 in vinyl compounds	CH out of plane deformation
1130.21	C-NH_2 in primary aliphatic amines	C-N stretch
1194.82	C=S in thiocarbonyl compounds	C=S stretch
1383.83	SO_2 in sulfonyl chlorides	SO2 antisym stretch
1562.23	NH in secondary amides	NH deformation
1648.06	N-H in primary amides	NH deformation
2881.45	CH_3 and CH_2 in aliphatic compounds	CH antisym and sym stretch
3299.01	NH_3^+ amino acids	NH_3^+ antisym stretch
3515.99	NH_2 in aromatic amines	NH stretch

3.4. XRD studies

XRD pattern taken using powder X-ray diffractometer instrument (XRDML) in the angle range of 10˚C-80˚C of the manganese nanoparticles at 2θ, scan axis: Gonio. A number of Bragg reflections corresponding to 28.33, 40.53 and 50.01 sets of lattice planes were observed which can be indexed to face-

centered cubic manganese (Fig.4 and Table-2). The peaks matched with the Joint Committee on Powder Diffraction Standards (JCPDS No. 04-0326), which further proved the formation of crystal manganese nanoparticles (Kumar *et al.*, 2012) [16]. The peaks were identified as manganese nanoparticles according to XPERT-PRO software (PDF#030921). The XRD pattern thus clearly showed that the manganese nanoparticles were crystalline in nature (Huang *et al.*, 1993) [17].

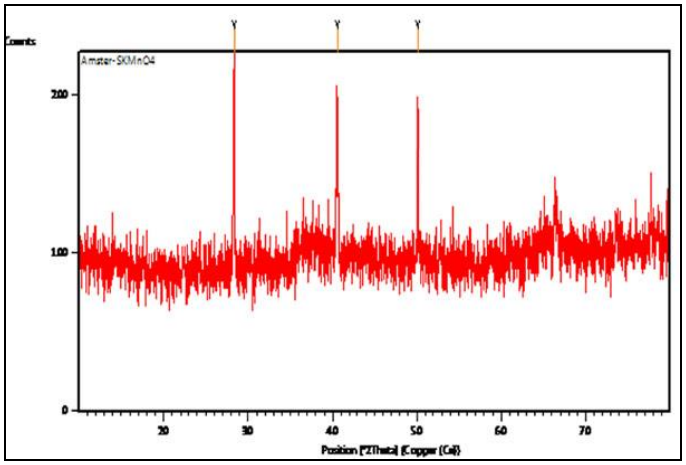

Fig 4: XRD analysis of MnNPs using *Ctenolepis garcinii* (Burm.f.) C.B. Clarke

Table 2: XRD peak value of MnNPs using *Ctenolepis garcinii* (Burm.f.) C.B. Clarke.

Pos. [°2Th.]	Height [cts]	FWHM Left [°2Th.]	d-spacing [Å]	Rel. Int. [%]
28.3376	132.59	0.1338	3.14951	100.00
40.5350	93.38	0.2676	2.22555	70.43
50.0195	82.8571	0.3238	1.79761	67.89

3.5. SEM and EDX analysis

Throughout the scanning range of binding energies, no peak belonging to impurity was detected. The results indicated that the reaction product was composed of highly pure manganese nanoparticles. A similar EDX spectrum (Fig.5) was obtained for each sample analyzed. Scanning electron microscopy provided further insight into the morphology and size details of the manganese nanoparticles. Comparison of experimental results showed that the diameter of prepared nanoparticles in the solution was about 57-69nm (Fig.6). The scanning electron micrographs of manganese nanoparticles obtained from the proposed bioreduction method at various magnifications.

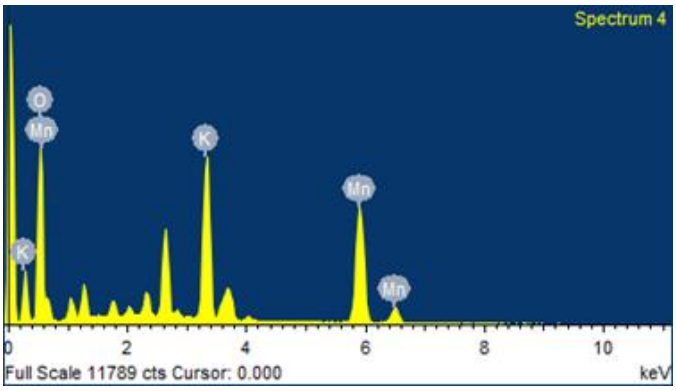

Fig 5: EDX spectrum of MnNPs using *Ctenolepis garcinii* (Burm.f.) C.B. Clarke.

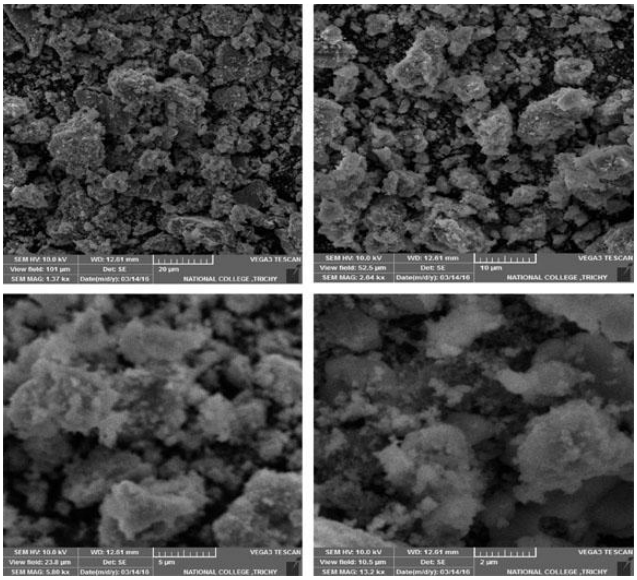

Fig 6: SEM image of MnNPs using *Ctenolepis garcinii* (Burm.f.) C.B. Clarke.

4. Conclusion

The aqueous extract of *Ctenolepis garcinii* (Burm. f.) C.B. Clarke was used to synthesis manganese nanoparticles. The manganese nanoparticles were characterized by UV-Visible Spectrophotometer, FT-IR, XRD, EDX and SEM. There is only one peaks at the centre at 415-417nm indicating the formation of manganese nanoparticles in elliptical shape using UV-Visible spectrophotometer. FT-IR spectrum of manganese nanoparticles showed the presence of bands at 513.03, 620.07, 989.41, 1130.21, 1194.82, 1383.83, 1562.23 1648.06, 2881.45, 3299.01 and 3515.99cm^{-1}. XRD pattern of manganese nanoparticles showed a number of Bragg reflections corresponding to ˚2 Theta of 28.33, 40.53 and 50.01 sets of lattice planes of manganese. EDX and SEM

analysis showed the impurities and the size of synthesized manganese nanoparticles about 57-69nm.

5. Reference

1. Lee SH, Salunke BK, Kim BS. Sucrose density gradient centrifugation separation of gold and silver nanoparticles synthesised using Magnolia kobus plant leaf extracts. Biotechnol. Bioproc, Eng. 2014; 19:169-174.
2. Kabir D, Altaf, Akram M. The kinetics of oxidation of L-tryptophan by water-soluble colloidal manganese dioxide. J. Disper. Sci. Technol. 2008; 29:809-816.
3. Gopidas KR, Whitesell JK, Fox MA. Synthesis, characterization and catalytic applications of a palladium-nanoparticle-cored dendrimer. Nano Lett. 2003; 3:1757-1760.
4. Sharma RK, Sharma P, Maitra A. Size-dependent catalytic behavior of platinum nanoparticles on the hexacyanoferrate (III)/thiosulfate redox reaction. J Colloid Interf. Sci. 2003; 265:134-140.
5. Boudjahem AG, Monteverdi S, Mercy M, Bettahar MM. Study of nickel catalysts supported on silica of low surface area and prepared by reduction of nickel acetate in aqueous hydrazine. J Catal. 2004; 221:325-334.
6. Moore JT, Corn JD, Chu D. Synthesis and characterization of a Pt3Ru1/Vulcan carbon powder nanocomposite and reactivity as a methanol electrooxidation catalyst. Chem. Mater. 2003; 15:3320-3325.
7. Nayak SK, Jena P. Equilibrium geometry, stability, and magnetic properties of small MnO clusters. J Am. Chem. Soc. 1999; 121(4):644-652.
8. Frattini A, Pellegri N, Nicastro D, Sanctis O. Effect of amine groups in the synthesis of Ag nanoparticles using aminosilanes. Mat. Chem. Phys. 2005; 94:148-152.
9. Iniya Udhaya C, John Peter Paul J, Amster Regin Lawrence R. Seaweed mediated biosynthesis of silver nanoparticles using Gracilaria fergusonii J Ag. collected from Hare Island, Thoothukudi in the south east coast of Tamil Nadu, India. International Journal of Plant Biotechnology. 2015; 1(2):17-24.
10. John Peter Paul J, Shri Devi SDK. Biosynthesis and characterization of silver nanoparticles using Gracilaria dura (AG.) J Ag. (Red seaweed). American Journal of PharmTech Research. 2014; 4(3):489-498.
11. Muthu Sheeba M, John Peter Paul J, Iniya Udhaya C. Green synthesis of silver nanoparticles using Enteromorpha linza (L.) J.Ag. (Green seaweed) from Hare Island, Thoothukudi, Tamil Nadu, India. European Journal of Molecular Biology and Biochemistry. 2014; 1(5):201-206.
12. Sakunthala M, Iniya Udhaya C, John Peter Paul J. Green synthesis of silver nanoparticles using Ctenolepis garcinii (Burm. f.) CB Clarke. European Journal of Biomedical and Pharmaceutical Sciences. 2017; 4(9):718-721.
13. Creighton JA, Eadont DG. Ultraviolet-visible absorption spectra of the colloidal metallic elements. Journal of Chemical Society Faraday Trans. 1991; 87:3881-3891.
14. Aoki FY, Macleod MD, Paggiaro P, Carewicz OEl, Sawy A, Wat C, *et al*. Early administration of oral oseltamivir increases the benefits of influenza treatment. J Antimicrob. Chemother. 2003; 51(1):123-129.
15. Kapoor. Hypoechoic periportal cuffing in acute myeloid leukemic. Journal of Clinical Ultrasound. 1998; 26(8):418-420.
16. Kumar M. Distribution of Lentinus tuberregium (Fr.), an indigenous edible medicinal mushroom in Tamil Nadu, South India. J Acad. Indus. Res. 2012; 1(6):297-302.
17. Huang CP, Dong CH, Tang Z. Advanced chemical oxidation: its present role and potential future in hazardous waste treatment. Waste Management. 1993; 13:361-377.